Mass of the lowest $T = 2$ state in ^{32}S: A test of the isobaric multiplet mass equation

S. Triambak,[1,2] A. García,[1] E. G. Adelberger,[1] G. J. P. Hodges,[1] D. Melconian,[1] H. E. Swanson,[1] S. A. Hoedl,[1] S. K. L. Sjue,[1] A. L. Sallaska,[1] and H. Iwamoto[1]

[1]*Physics Department, University of Washington, Seattle, Washington 98195-1560, USA*

[2]*Department of Physics, University of Notre Dame, Notre Dame, Indiana 46556, USA*

(Received 11 January 2006; published 22 May 2006)

We produced the lowest $T = 2$ state in ^{32}S with the ^{31}P(p, γ) reaction and measured the energies of the deexcitation γ rays, obtaining an excitation energy of 12047.96 ± 0.28 keV that disagrees with a previous value of 12045.0 ± 0.4 keV. Our result, together with a recent measurement of the ^{32}Ar mass, makes the A = 32 multiplet the most precisely measured $T = 2$ quintet and provides easily the most stringent test of the isobaric multiplet mass equation. A significant violation of the isobaric multiplet mass equation is observed that could be explained by mixing with a nearby $T = 0$ level.

DOI: 10.1103/PhysRevC.73.054313 PACS number(s): 21.10.Dr, 21.10.Hw, 23.20.Lv, 27.30.+t

I. INTRODUCTION

If the nucleon-nucleon interaction were charge independent, the $2T + 1$ members of an isospin multiplet would have identical masses. However, this degeneracy is broken by charge-dependent interactions between the nucleons which have the general form

$$H_c = \sum_{i<j} (\alpha \tau_z(i) + \beta)(\alpha \tau_z(j) + \beta) f(r_{ij}), \tag{1}$$

where τ is the nucleon isospin operator and α and β are constants that depend on the nature of the charge-dependent interaction. This Hamiltonian is a sum of isoscalar, isovector, and isotensor operators. Therefore, at tree-level, the masses of the $2T + 1$ members of the isobaric multiplet should obey the isobaric multiplet mass equation (IMME) [1,2]

$$M(T_z) = \mathrm{a} + bT_z + cT_z^2, \tag{2}$$

where $T_z = (Z - N)/2$, the z component of total isospin T, ranges from $-T$ to $+T$. Summaries of existing data on isobaric multiplets can be found in Refs. [3,4]. The only significant deviations are found in light nuclei with unbound states. The $A = 9$, $T = 3/2$ quartet requires an additional cubic term and has been explained as a combination of higher order charge-dependent interactions and expansion of the nuclear wave function due to Coulomb effects [5]. The $A = 8$, $T = 2$ quintet requires either an additional dT_z^3 term or a eT_z^4 term or both for a satisfactory fit. Although no fundamental principle forbids violation of Eq. (2), theoretical calculations [6] indicate that the IMME should hold down to $\approx$1 keV for multiplets that do not have isospin-allowed strong decays. This has made it a useful tool for estimating masses of proton-rich members of multiplets where direct measurements are difficult.

The lowest $A = 32$, $T = 2$ multiplet has the most precisely measured masses of any isospin quintet [3]. However the mass of the $T_z = 0$ member of the multiplet stands on a weak footing. A ^{31}P(p, α) resonance study [7] gave an excitation energy of 12049 ± 2 keV. An earlier ^{31}P(p, γ) study [8] obtained a significantly different result, i.e., an excitation energy of 12045.0 ± 0.4 keV, but no details were provided about the difficult task of determining the excitation energy to such a high precision. This motivated us to remeasure the excitation energy of the lowest $T = 2$ state of ^{32}S using the ^{31}P(p, γ) reaction.

II. EXPERIMENTAL PROCEDURE

A. Apparatus

Our ^{31}P(p, γ) measurement was performed with the University of Washington FN tandem accelerator, operating in a mode with the ion source at the terminal. We produced the ^{31}P target by implanting 55 μAh of 90 keV ^{31}P ions from a sputter ion source into a 0.5 mm thick tantalum backing. The ^{31}P beam was rastered using computer-controlled magnetic steerers to produce a uniform target with a cross section of approximately 1.1 cm^2 and a measured energy loss of 4 keV for 3 MeV protons. A 6 μA, 3.285 MeV proton beam bombarded the water-cooled ^{31}P target to produce the lowest $T = 2$ state in ^{32}S. This level, as shown in Fig. 1, mainly γ decays to a $J^\pi = 1^+$, $T = 1$ state at $\approx$8 MeV, which in turn decays to the ground state with a high branching ratio [9]. Gamma rays were registered with a 50% HPGe (GMX) detector whose signals were processed by temperature-controlled electronics to minimize gain drifts. We made two independent measurements at two different times. In the first, we took data with two HPGe detectors located $\approx$60 cm from the center of the chamber, at $\pm 90^\circ$ to the beam where the Doppler shift is minimal. The energy calibration was based on a ^{56}Co source and ^{35}Cl(n, γ) capture radiation. In the second measurement, the detector was aligned at 0° as shown in Fig. 2 and positioned 10.3 cm from the target. Although Doppler shifts are maximum at $\theta_\gamma = 0^\circ$, it gave the least sensitivity to detector mis-alignment. The energy calibration for this measurement was based on ^{56}Co and ^{27}Al(p, γ) radiation. Figure 3 shows a gamma spectrum from the 0° experiment.

B. Energy calibration

A ^{56}Co source, present at all times during data acquisition, provided γ-ray calibrations with energies up to 3.5 MeV. Calibration points with higher energies were obtained from

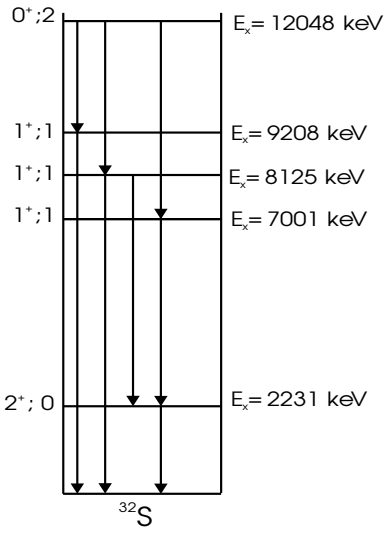

FIG. 1. Gamma decays of the lowest $T = 2$ state in ^{32}S.

capture reactions. Gamma rays with well-known energies up to 10762 keV [10] were generated by bombarding a 20 μg/cm^2 thick ^{27}Al target with a 15 μA, 992 keV proton beam. Gamma rays with well-determined energies up to 8.5 MeV were produced with the ^{35}Cl(n, γ) reaction [11]. For this calibration, the ^{31}P target was removed and a thick ($\approx$500 μg/cm^2) Li_2O target evaporated on a Ta backing was placed at the edge of the target chamber and bombarded by a 600 nA, 1.912 MeV proton beam, producing ^{7}Li(p, n) neutrons in a forward-angle cone, with a nearly Maxwellian velocity distribution for neutron energies between 0 and 110 keV [12]. The neutrons were moderated by a 4 cm thick paraffin slab before capturing onto a 8×10^3 cm^3 volume of NaCl. The HPGe detector was moved to an angle of 90° approximately 60 cm from the center of the chamber at shown in Fig. 4. Neutrons moving toward the Ge detector were attenuated by 8 cm of paraffin followed by 15 cm of borax to protect the detector from neutron damage. Figure 5 shows typical calibration spectra.

III. DATA ANALYSIS

Incomplete charge collection within Ge detectors produces exponentially decaying tails below gamma-ray peaks [13,14] while multiple-Compton scattering gives plateaus below the peak centroid. We extracted peak centroids by fitting our γ peaks with a Gaussian folded with a delta function and two

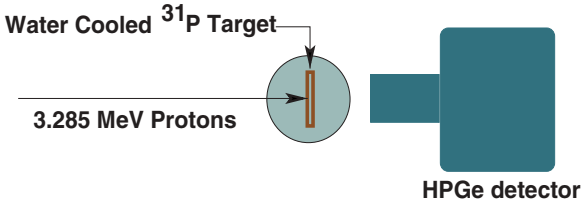

FIG. 2. (Color online) Top view of the experimental setup used for the ^{31}P(p, γ) data.

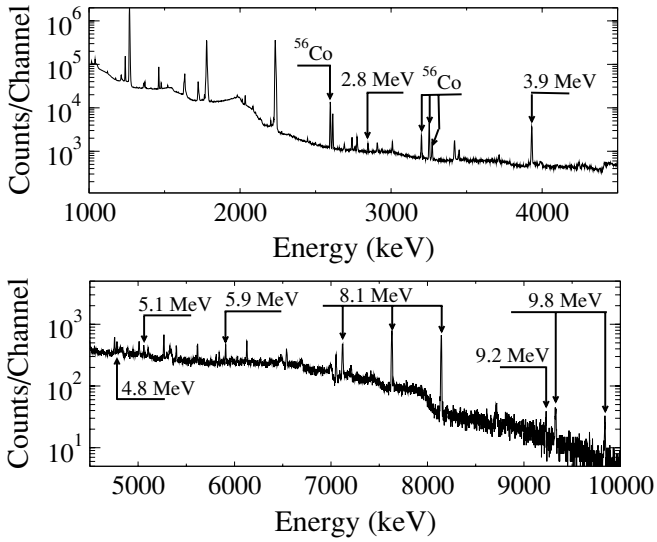

FIG. 3. ^{31}P(p, γ) spectrum from the 0° experiment. The ^{32}S lines and some ^{56}Co calibration peaks are labeled. The 9.8 MeV γ ray is mainly from direct capture.

low-energy exponential tails. Each tail had the form

$$T(x) = \frac{1}{2l}\exp\left[\frac{(x-\mu)}{l} + \frac{1}{2}\left(\frac{\sigma}{l}\right)^2\right] \times \mathrm{erfc}\left[\frac{1}{\sqrt{2}}\left(\frac{(x-\mu)}{\sigma} + \frac{\sigma}{l}\right)\right], \quad (3)$$

where erfc is the complementary error function, $l$is the decay-length of the tail, σ is the Gaussian spread and μ is the peak centroid. The γ-peak line-shapes were assumed to have the form

$$R = T_1 f_1 + T_2 f_2 + \frac{1}{\sqrt{2\pi\sigma^2}}\exp\frac{-(x-\mu)^2}{2\sigma^2}, \quad (4)$$

where f_1 and f_2 were the relative areas of the exponentials with respect to the pure Gaussian.

We first determined the line-shape of a high-statistics 3253 keV peak from ^{56}Co by keeping the decay length of

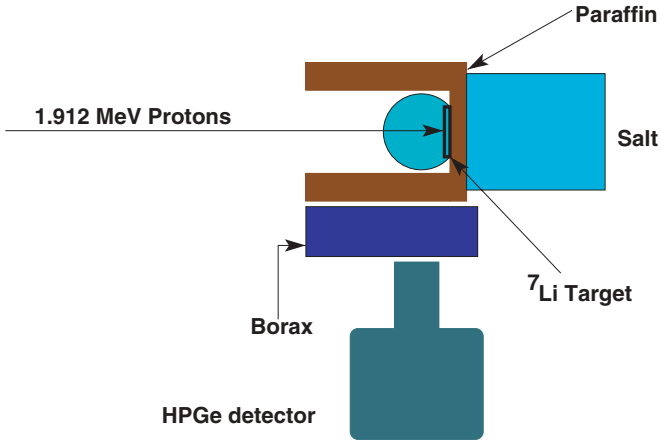

FIG. 4. (Color online) Top view of the experimental setup for the ^{35}Cl(n, γ) calibration used in the $\theta_\gamma = \pm 90°$ measurement.

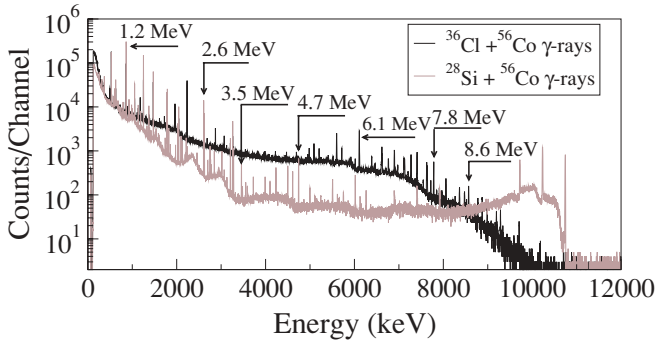

FIG. 5. (Color online) Calibration lines with detector postioned at 90° to the beam.

the second tail l_2, representing the multiple-Compton plateau below the centroid, at a large and fixed value (≈460 keV) and varied the remaining parameters and the background to minimize χ^2. We then fitted the other gamma peaks by requiring l_1 and f_1 to scale linearly with energy while varying the other parameters to minimize χ^2. Peaks on Compton edges of other γ rays were avoided so that we could fit using a flat backgound. Figure 6 shows the gamma rays of interest and their fits.

We minimized sensitivity to ADC nonlinearities and line-shape variations by the following procedure. The centroids, x_i, of a few calibration gamma-ray peaks around each ^{31}P(p, γ) line of interest were fitted to a linear function, $E_{\gamma i} = a + bx_i$. The uncertainties in peak centroids were obtained by combining in quadrature the errors due to counting statistics and to uncertainties in the calibration energies. This gave us the a and b coefficients which related the ^{31}P(p, γ) energies to the closest calibration line,

$$E_{\gamma i}(^{32}\mathrm{S}) = E_{\gamma i}(\mathrm{cal}) + b \times [x_i(^{32}S) - x_i(\mathrm{cal})]. \qquad (5)$$

IV. SYSTEMATIC EFFECTS

A. Gain drifts

Although we used a temperature-controlled electronics rack, Fig. 7 shows that small gain drifts did occur.

We corrected for these drifts using a time stamp that was recorded for each event. Corrections, based on a few high-

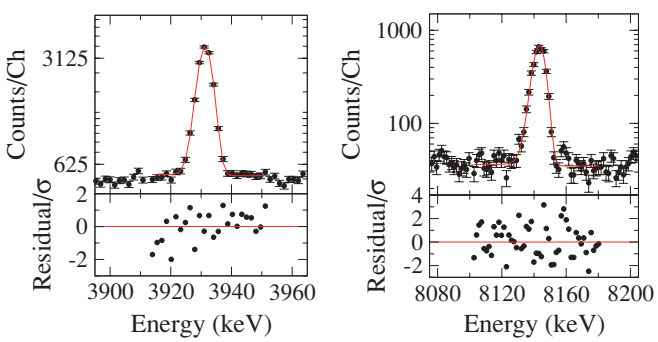

FIG. 6. (Color online) Fits to the most intense deexcitation gamma-rays from the $T = 2$ state.

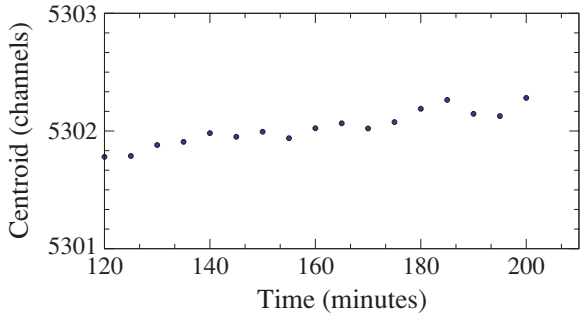

FIG. 7. (Color online) Centroid of the 2598 keV ^{56}Co γ peak as a function of time.

statistics peaks, were applied piecewise to data taken over time intervals ranging between 15 and 180 mins. These calibrations were used to match the centroids of the shifted events to a fixed reference.

B. ADC nonlinearities

Detector signals were digitized by an Ortec 413 ADC. We observed significant nonlinearity in the energy range $0 \leqslant E_\gamma \leqslant 1.5$ MeV (see Fig. 8) and did not use any lines in that range for gain-matching or energy determination. Additional data, taken with the doubled gains in the spectroscopy amplifiers, proved that the nonlinearity was a property of the ADC and not of the preceding electronics; these data also provided an additional check on the energy of the 3.9 MeV ^{31}P(p, γ) gamma ray.

C. Doppler shifts

Although the Doppler shifts are minimal at $\theta_\gamma = \pm 90°$, the sensitivity to angular uncertainty is maximal. It is unlikely that our detectors and target could be misaligned by as much as 0.5 cm, and a very conservative estimate of the upper limit of the detector and target misalignment was ≈1.0 cm. Monte Carlo calculations simulated Doppler-shifts of γ-ray energies, taking into consideration detector mis-alignment and recoil slowing. Doppler shifts of ^{31}P(p, γ) and ^{27}Al(p, γ) gammas were simulated using the half-life of the decaying

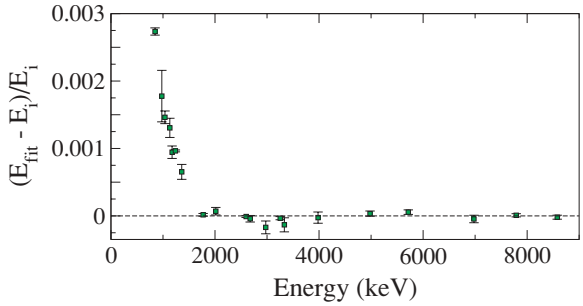

FIG. 8. (Color online) Nonlinearity of the ADC. The points show centroids of ^{35}Cl(n, γ) and ^{56}Co calibration lines. Pronounced differences are seen between the observed positions and a linear fit to the region between 2015 and 8578 keV.

TABLE I. Predicted Doppler-shifts.

Source	E_γ (keV)	Detector distance (cm)	Detector angle (deg)	Doppler shift (keV)
^{31}P(p,γ)	3922	10.3 ± 1.0	$0^\circ \pm 5.55^\circ$	10.06 ± 0.07[a]
		59.0 ± 1.0	$90^\circ \pm 0.97^\circ$	0.00 ± 0.17
^{31}P(p,γ)	8124	10.3 ± 1.0	$0^\circ \pm 5.55^\circ$	20.83 ± 0.13[a]
		59.0 ± 1.0	$90^\circ \pm 0.97^\circ$	0.00 ± 0.36
^{27}Al(p,γ)	7922	10.3 ± 1.0	$0^\circ \pm 5.55^\circ$	12.30 ± 0.08[a]
^{35}Cl(n,γ)	8578	59.0 ± 1.0	$90^\circ \pm 0.97^\circ$	-0.23 ± 0.20

[a]A simple estimate assuming zero lifetime for the parent state and zero detector solid angle yields shifts of 10.3, 21.3 and 12.6 keV, respectively, for the 3922, 8124, and 7922 keV γ rays.

state to randomly generate decay times from an exponentially decaying distribution. The energy loss by the compound nucleus during that lifetime was calculated using the stopping power at that particular energy (which was determined by using SRIM [15]). For the ^{27}Al(p,γ) energy calibration we used only the primary gammas emitted by the parent $Ex = 12541.31$ keV state. Doppler broadenings of the secondary gammas from ^{31}P(p,γ) were simulated by accounting for the angular-correlation between the two emitted gammas as well as the transverse component of momentum imparted by the emission of the first gamma ray.

For the ^{35}Cl(n,γ) reaction, the neutron angular-distribution results for ^{7}Li(p,n) from Ref. [12] were fed into a program that simulated neutron scattering on paraffin and neutron capture on ^{35}Cl. This simulation provided us with the eventual recoil velocities of the ^{36}Cl nuclei prior to γ emission. The recoil velocities and directions, and the known γ energies from Ref. [11], were entered into the radiation-transport program PENELOPE [16] to simulate the interaction of the γ radiation with the detector and calculate the net Doppler shift. The results are shown in Table I. Although the corrections for the 0° data are large, their model-dependence is very small because the shifts were virtually unattenuated; in all the cases the ions changed their velocities by $<10^{-7}\,c$ during the parent state's lifetime.

D. Field-increment effect

Acceleration of primary and secondary charge carriers within the intrinsic volume of the detector, and variations in the charge collection efficiency over the detector volume, can shift the observed peaks in a manner that depends on source position, detector geometry, bias voltage and γ-ray energy [17]. It was important to test the magnitude of this effect in our measurement because the γ rays from the ^{31}P(p,γ) and ^{27}Al(p,γ) reactions were at $\approx 0^\circ$ to the detector, whereas the ^{35}Cl(n,γ) γ-rays were incident on the detector from the side (see Fig. 4).

We tested the magnitude of this effect by fixing a ^{56}Co source at 0° to the detector 5 cm from the detector end-cap. We then took ^{35}Cl(n,γ) data with the Ge detector at 65°, 90°, and 125° to the beam at the center of the chamber. This ensured that the ^{36}Cl γ rays were incident on the detector at three different angles, while gammas from the ^{56}Co source were always from a fixed postion. The energies of the ^{35}Cl(n,γ) lines were corrected for Doppler shifts as described above. Figure 9 shows the difference between the Doppler-shift-corrected data at 125° and 65°. A small systematic effect may be present, but it was not large compared to our other uncertainties. The shifts are relatively insignificant for high energies.

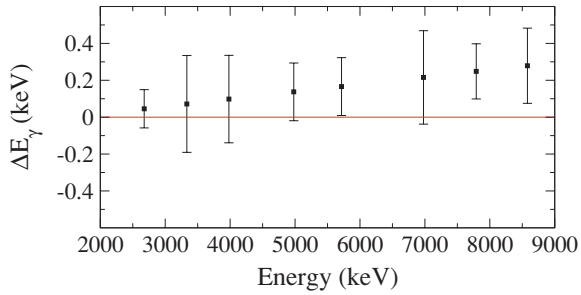

FIG. 9. (Color online) Shifts in apparent γ-ray energies with changes in the incident γ-ray angle. The y-axis shows the difference in the inferred Doppler-shift-corrected γ energies from ^{35}Cl(n,γ) at two extreme angles (incident along the axis of the co-axial detector and approximately normal to the detector axis). A ^{56}Co source fixed to the detector provided a angle-independent reference.

E. Nonresonant background

If there were a nonresonant component to the 3922 and 8124 keV γ-rays it would shift their centroids in manner depending on the beam energy and the structure of our target. We found no evidence for such nonresonant components.

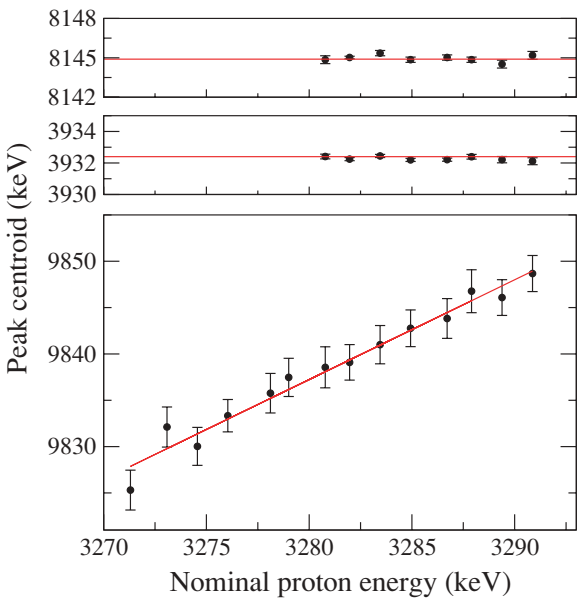

FIG. 10. (Color online) Energies of the 3.9 and 8.1 MeV γ peaks versus proton energy in the lab frame. For comparison we show the γ_1 data which shows a non-resonant behavior as expected. The energies of the 3.9 and 8.1 MeV γ peaks were obtained from line-shape fits, while the γ_1 energies are simple centroids. Data points at lower proton energies are missing for the 3.9 and 8.1 MeV gammas because there are no observable peaks.

TABLE II. Level energies and Doppler-corrected γ-ray energies from ^{32}S.

J^π, T	Ex (keV)		E_γ (keV)[e]
	Previous work	This work	
$2^+, 0$	2230.57(15)[a]	. . .	. . .
$1^+, 1$	7002.5(10)[b]	7001.44(36)	4770.49(33)
$1^+, 1$	8125.40(20)[a]	8125.32(24)[d]	5894.32(28)
			8124.12(24)
$1^+, 1$	9207.5(7)[b]	9207.55(71)	9206.13(71)
$0^+, 2$	12045.0(4)[c]	12047.96(28)	2840.32(14)
			3922.37(15)
			5046.09(39)

[a]From Ref. [18].
[b]From Ref. [27].
[c]From Ref. [8].
[d]Weighted mean of the excitation energy obtained using the 5894-2230 keV cascade and the 8124 keV γ ray.
[e]Obtained from a weighted mean of the 0° and the 90° data. The uncertainties are from the 0° data.

Figure 10 shows the centroids of 3922 and 8125 keV γ rays versus proton energy from the 0° detector. For comparison we show the centroid for the γ_1 yield, which does not come from a narrow resonance.

V. RESULTS AND DISCUSSION

A. Excitation energy of the $T = 2$ state

The precision of the ±90° data was limited both by possible mis-alignments of the Ge detectors and by the incident-angle dependence of the pulse height in the ^{36}Cl calibration.

Table II compares our results to previous studies. We agree well with previous determinations of the excitation energies of the three $T = 1$ levels fed in by the $T = 2$ state, but not with the previously cited value [8] for the excitation energy of the $T = 2$ state itself. Table III shows the gamma energies in the three cascade chains observed in this work and the deduced excitation energy of the $T = 2$ level. Our value for the excitation energy of the lowest $T = 2$ state, 12047.96(28) keV, is about 3.0 keV ($\approx 7\sigma$) higher than that reported by Antony *et al.* [8] but agrees well with the lower-precision results of Ref. [7].

TABLE III. Gamma-ray energies for cascades from the lowest $T = 2$ state in ^{32}S.

$E_{\gamma 1}$ (keV)	$E_{\gamma 2}$ (keV)	Ex (keV)
5046.09(39)	4770.49(33)[a]	12047.96(53)
3922.37(15)	8124.12(24)	12047.86(28)
3922.37(15)	5894.32(28)[a]	12048.10(35)
2840.32(14)	9206.13(71)	12048.01(72)
Combined value[b]		12047.96(28)

[a]This γ-ray deexcites to the first excited state. We used the excitation energy of the first excited $E_{x1} = 2230.57(15)$ keV from Ref. [18] to obtain E_x of the $T = 2$ state.
[b]Because the uncertainties are correlated we use the smallest of the uncertainties in the above data as the total uncertainty in the excitation energy.

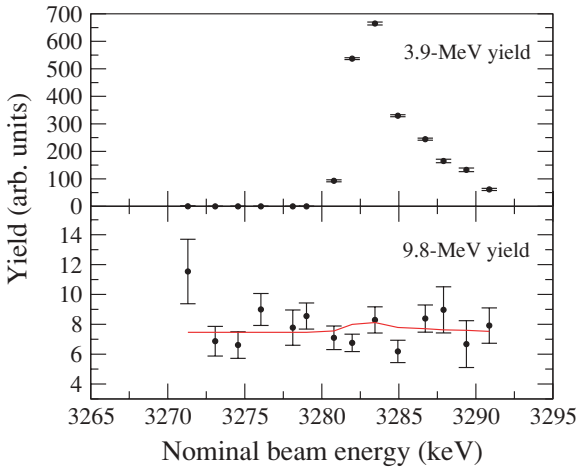

FIG. 11. (Color online) Top panel: Excitation function of 3922-keV γ yield. Bottom panel: Excitation function of γ_1 yield (this includes the single escape peak for additional statistics). The continuous line shows the upper limit described in the text.

B. Isospin-violating γ decays

The ^{32}S $T = 2$ state provides a clean test of the isospin selection rule that $\Delta T = 0, 1$ in γ decays. We tested this by searching for a resonant component in the $\Delta T = 2$ γ_1 transition.

A previous measurement showed a flat background for the γ_1 yield [19]. Figure 11 shows our γ_1-yield excitation function, as well as the excitation function for the 3922-keV γ ray. We fitted the γ_1 yield to a constant plus a resonant term which we assumed had the same shape as the 3922-keV γ yield. The best fit gave a resonant contribution consistent with zero. By calculating the likelihood function as we varied the magnitude of the resonant term we obtain an upper limit on the branch to the 2.231 MeV state of 0.25% at the 90% confidence level. Table IV shows the relative γ branches of the $A = 32$, $T = 2$ states. Our measured strength ratio $\Gamma_\gamma(T = 2 \rightarrow 2231)/\Gamma_\gamma(T = 2 \rightarrow 8125)$ when expressed as an $E2/M1$ ratio of Weisskopf reduced strengths is less than 0.9%.

TABLE IV. Relative gamma branches (in %) from the lowest $A = 32$ $T = 2$ states. Excitation energies are in keV.

Final st.	^{32}P		^{32}S		
$J^\pi_n;T$	Ex	Ref. [24]	Ex	Ref. [9]	This work[a]
$1^+_3;1$	2230	9.4(5)	9208	11(2)	9.4(7)
$1^+_2;1$	1149	85.7(8)	8125	83(8)	84.3(9)
$1^+_1;1$	0	4.7(6)	7001	6(1)	6.3(7)
$2^+_1;0$	N/A	N/A	2231	$\leqslant 0.8$	$\leqslant 0.25$

[a]We assumed a 6% uncertainty in the ratio of γ-detection efficiencies.

TABLE V. Comparison of the measured mass excesses of the lowest $T = 2$ quintet in $A = 32$ with a fit to the isospin-multiplet mass equation.

Isobar	T_z	M_{Exp} (keV)[a]	M_{IMME} (keV)
^{32}Si	−2	−24080.86 ± 0.77[b]	−24082.52 ± 0.61
^{32}P	−1	−19232.78 ± 0.20[c]	−19232.48 ± 0.18
^{32}S	0	−13967.74 ± 0.31[d]	−13968.32 ± 0.26
^{32}Cl	+1	−8291.5 ± 1.8[e]	−8290.05 ± 0.63
^{32}Ar	+2	−2200.2 ± 1.8[f]	−2197.67 ± 1.50
		$Q(\chi^2 = 13.1, \nu = 2)$[g] = 0.001	

[a]Unless noted otherwise, ground state masses are from Ref. [23].
[b]From Ref. [20].
[c]$E_x = 5072.44 \pm 0.06$ keV from Ref. [24].
[d]This work.
[e]Pyle *et al.* [25].
[f]Blaum *et al.* [26].
[g]$Q(\chi_0^2, \nu)$ is the probability of obtaining a set of data with $\chi^2 \geqslant \chi_0^2$, given that the model is correct.

C. A test of the IMME

We combine our ^{32}S results with the best available results for the other four members of the $A = 32$ isospin multiplet to obtain the most precisely measured isospin quintet. We used Ref. [20] for the ^{32}Si mass rather than the more precise value from the latest compilation [23] because we are uncomfortable adopting an uncertainty ≈15 times smaller than that quoted by the experimenters themselves. Because of the high precision attained in this multiplet, a new measurement of the ^{32}Si mass would be welcome as the existing mass measurements are not well documented [20,21]. We fit these results to the IMME in Table V and Fig. 12 and observe a significant disagreement with the IMME prediction, $Q(\chi^2, \nu) = 0.001$. Reasonable agreement with the data, $Q(\chi^2, \nu) = 0.21$, can be found by adding a very small cubic term, dT_z^3 to Eq. (2) with $d = 0.54 \pm 0.16$ keV, which is the smallest known and most precisely determined violation of the IMME. For comparison, the most precise previous determination of a d coefficient had an uncertainty of 1.4 keV [3]. Fitting the data with a quartic, rather than cubic, term, gives a quartic coefficient, $e = 0.53 \pm 0.15$ keV; with $Q(\chi^2, \nu) = 0.64$.

The only significant difference on using Ref. [23] for the ^{32}Si mass instead of Ref. [20] is that we obtain a much larger disagreement with the IMME, $Q(\chi^2, \nu) = 5 \times 10^{-5}$. The d and e coefficients are consistent with those we quote, with slightly smaller uncertainties. The conclusions that follow are unaffected.

Our result provides the best demonstration of the validity of the approximations inherent in the IMME and its utility for predicting masses away from the valley of stability. The larger violations of the IMME observed in the very light nuclei [3] probably arise from the less tightly bound nature and smaller Coulomb barriers of those states, which lead to nonperturbative effects.

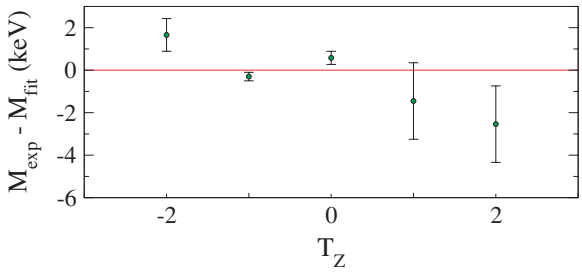

FIG. 12. (Color online) Difference between measured mass excesses and IMME fit for the $A = 32$, $T = 2$ quintet in keV.

Excellent agreement with the IMME in the $A = 32$ system, $Q(\chi^2, \nu) = 0.74$, would be obtained if the excitation energy of the $T = 2$ state in ^{32}S were 2.5 keV lower than we find. Could this be explained by isospin mixing? A $\Delta T = 2$ $E2$ transition from the $T = 2$ state to the first excited $J^\pi = 2^+$, $T = 0$ state at 2.2 MeV would be evidence for such mixing. However, we saw no evidence for this transition. This, however does not rule out the mixing scenario. Two 0^+ levels are known [27] to lie slightly below the $T = 2$ state and are candidates for the admixed level.

A 100 eV wide $J^\pi, T = 0^+, 0$ level at $Ex = 11930$ keV lies 118 keV below the $T = 2$ state. An isospin-mixing matrix element of ≈17 keV would shift the $T = 2$ state upward by 2.5 keV, implying an isospin impurity with an intensity of 2.1%. This $J^\pi, T = 0^+, 0$ level would not affect the positions of the $T = 2$ states in ^{32}P and ^{32}Cl, which is consistent with the data. A second $J^\pi = 0^+$ level (of unknown isospin) occurs at $Ex = 11869$ keV. If this level were responsible for the 2.5 keV shift, it would need a mixing matrix element of 21 keV and an isospin impurity with an intensity of 1.4%. Matrix elements of this size are not implausible.

We measured excitation functions around both the 11930 and 11869 keV resonances and found no resonant component to the γ_1 yield on the first resonance and a significant yield on the second. Assuming $\Gamma_p/\Gamma = 1$ in all cases, the $T = 2$, 11930 keV and 11869 keV states have γ_1 widths of $\leqslant 7.3$, $\leqslant 52$ and 330(70) meV. These results do not exclude either of the levels as the source of the isospin admixture.

ACKNOWLEDGMENTS

We thank Kurt Snover for illuminating comments. We are grateful to Doug Will and Abhishek Kulkarni for help in target preparation and Greg Harper for help with accelerator operations. We also thank the U.S. Department of Energy for support.

[1] E. P. Wigner, *Proceedings of the Robert A. Welch Conferences on Chemical Research, Houston* (Robert Welch Foundation, Houston, 1957), Vol. 1.
[2] S. Weinberg and S. B. Treiman, Phys. Rev. **116**, 465 (1958).
[3] J. Britz, A. Pape, and M. Antony, At. Data Nucl. Data Tables **69**, 125 (1998).
[4] W. Benenson and E. Kashy, Rev. Mod. Phys. **51**, 527 (1979).
[5] G. Bertsch and S. Kahana, Phys. Lett. **B33**, 193 (1970).

[6] E. M. Henley and C. E. Lacy, Phys. Rev. **184**, 1228 (1969).
[7] J. F. Wilkerson *et al*., Nucl. Phys. **A549**, 223 (1992).
[8] M. S. Antony *et al*., *Proceedings of the International Conference on Nuclear Physics, Berkeley, 1980* (Lawrence Berkeley Laboratory, Berkeley, CA, 1980), Vol. 1.
[9] J. Vernotte, S. Gales, M. Langevin, and J. M. Maison, Phys. Rev. C **8**, 178 (1973).
[10] P. M. Endt *et al*., Nucl. Phys. **A510**, 209 (1990).
[11] B. Krusche *et al*., Nucl. Phys. **A386**, 245 (1982).
[12] W. Ratynski and F. Käppeler, Phys. Rev. C **37**, 595 (1988).
[13] R. G. Helmer, J. E. Cline, and R. C. Greenwood, in *The Electromagnetic Interaction in Nuclear Spectroscopy*, edited by W. D. Hamilton (North-Holland Publishing Company, Oxford, 1975), p. 775.
[14] T. Katou, Nucl. Instrum. Methods **124**, 257 (1975).
[15] http://www.srim.org/.
[16] J. Sempau *et al*., Nucl. Instrum. Methods Phys. Res. B **132**, 377 (1997).
[17] R. G. Helmer, R. J. Gehrke, and R. C. Greenwood, Nucl. Instrum. Methods **123**, 51 (1975).
[18] M. Babilon, T. Hartmann, P. Mohr, K. Vogt, S. Volz, and A. Zilges, Phys. Rev. C **65**, 037303 (2002).
[19] K. A. Snover, Ph.D. thesis, Stanford University, (1969).
[20] A. Paul, S. Röttger, A. Zimbal, and U. Keyser, Hyperfine Interact. **132**, 189 (2001).
[21] Reference [23] calculated the mass from the ^{31}Si(n, γ) gamma-ray energy published in Ref. [22], but corrected the unreasonable published uncertainty of 0.0005 keV to 0.05 keV by studying how well other known γ-ray energies were reproduced. However, the authors of Ref. [22] themselves presented a revised evaluation of the mass of ^{32}Si with an uncertainty of 0.822 μu or 0.77 keV [20].
[22] S. Röttger, A. Paul, and U. Keyser, IEEE Trans. Instrum. Meas. **46**, 560 (1997).
[23] G. Audi, A. H. Wapstra, and C. Thibault, Nucl. Phys. **A729**, 337 (2003).
[24] P. M. Endt, Nucl. Phys. **A521**, 1 (1990).
[25] M. C. Pyle *et al*., Phys. Rev. Lett. **88**, 122501 (2002).
[26] K. Blaum, G. Audi, D. Beck, G. Bollen, F. Herfurth, A. Kellerbauer, H. J. Kluge, E. Sauvan, and S. Schwarz, Phys. Rev. Lett. **91**, 260801 (2003).
[27] http://www.nndc.bnl.gov